UNIVERSITAT DE BARCELONA

Quantum Nanomagnetism and applications

Professor Javier Tejada.
Dept. Física Fonamental, Universitat de Barcelona.

XLVIII Zakopane School of Physics
May 22nd, 2013

UNIVERSITAT DE BARCELONA

Content

Introduction to magnetism

Single Domain Particles

Resonant spin tunneling on Molecular Magnets

Quantum magnetic deflagration

Superradiance

Rotational Doppler Effect

2d magnetic vortices

Quantum tunneling of N-SC interfaces

Introduction to magnetism

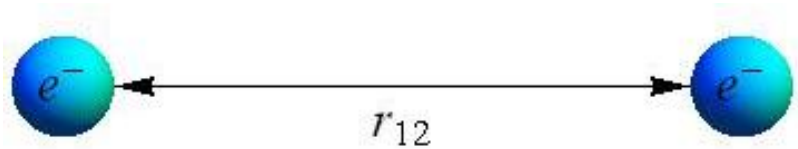

- Electrostatic interaction + Quantum Mechanics

$$\frac{e^2}{r_{12}}$$

Overlapping of wave functions

$$\left\langle \frac{e^2}{r_{12}} \right\rangle$$ Is different for $S=0$ and $S=1$

Term $\boldsymbol{s}_i \cdot \boldsymbol{s}_j$ in the Hamiltonian → Heisenberg hamiltonian

Exchange interaction

Atoms can be found with two or more interacting electrons. Considering two of them in an atom, the energy of the spin interaction can be calculated:

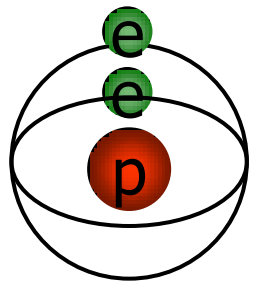

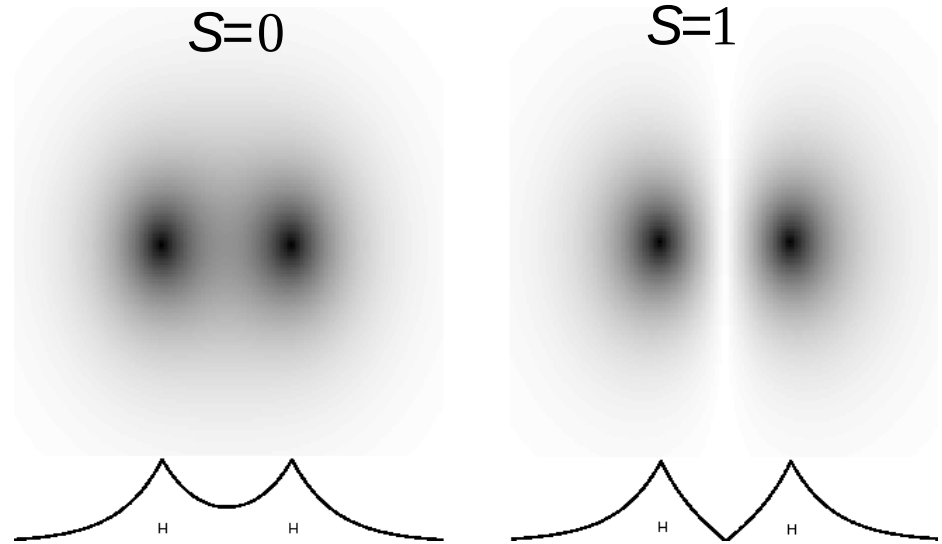

The system always tends to be at the lowest energy state: $J \sim T_c$

$$\mathcal{H}_{ex} = -\sum_{i<k} J(r_{ik})\, \boldsymbol{s}_i \cdot \boldsymbol{s}_k \longrightarrow \mathcal{H}_H = -\sum_{\langle i<k \rangle} J_{ik}\, \boldsymbol{s}_i \cdot \boldsymbol{s}_k \Rightarrow \hat{\mathrm{H}}_{eff} = -J\hat{\vec{S}}_1 \cdot \hat{\vec{S}}_2$$

The overlapping of the wave functions decays exponentially.

Summation over nearest neighbours

Magnetic anisotropy

It comes from the coupling between the electronic spins and the magnetic field induced by the electrostatic crystal field (along their orbital motion)

- Relativistic origin: effect proportional to $\left(\frac{v}{c}\right)^p$, with *p* even.
- Classical description: energy barrier of height

$$U = kV \qquad \Rightarrow \Gamma \approx e^{(-U(V)/T)}$$

Anisotropy constant

Volume

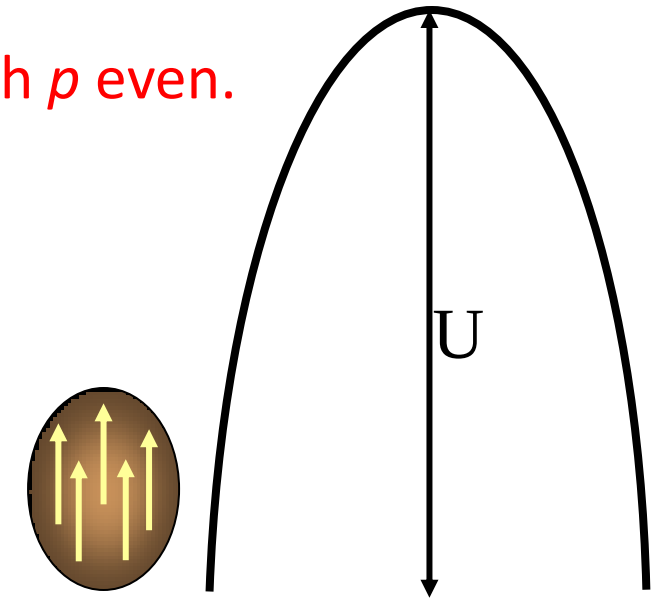

- Quantum description: crystal-field hamiltonian

$$\mathcal{H}_A = \frac{1}{2}\sum_n S_{n\alpha}S_{n\beta} + \frac{1}{4}c_{\alpha\beta\gamma\delta}\sum_n S_{n\alpha}S_{n\beta}S_{n\gamma}S_{n\delta} + \ldots$$

where S_n is the spin of a microscopic volume.

Single domain particles (SDP)

- Domains and domain walls:

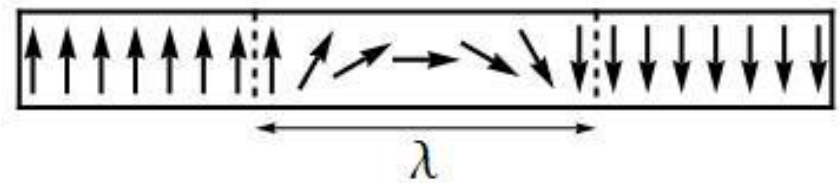

- Tipically $\frac{E_{ex}}{E_{an}} \approx 10^3 - 10^5$ → The exchange energy is so high that it is difficult to do any non-uniform rotation of the magnetization ($\lambda \sim nm$).

- If the particle has $R < \lambda$ then no domain wall can be formed. This is a SDP:

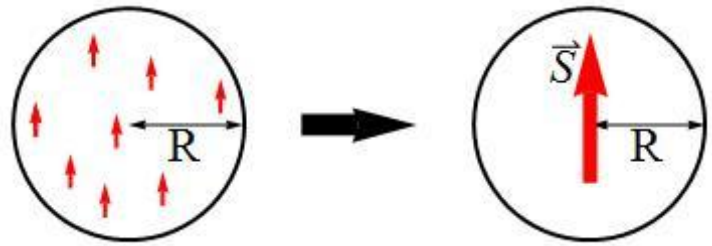

- The probabilty of an individual spin flip is:

$$\Gamma \sim \exp\left(-E_{ex}/T\right) \to 0 \quad \text{with} \quad E_{ex} \sim T_C$$

Hence, at low T, the magnetic moment is a vector of constant modulus:

$$T \ll T_C \Rightarrow |\vec{S}| = ct$$

SDP: magnetic relaxation

- The particles relax toward the equilibrium state:

$$M = M_0 \left(1 - S \ln(t/\tau_0)\right)$$

Initial magnetization — **Viscosity** — Microscopic attempt time

- The dependence of *S* on *T* shows two different regimes:
  1) **Thermal regime**: at high temperatures it is easier to "jump" the barrier. In this regime, $S \mu T$
  2) **Quantum regime**: at low temperatures, magnetic relaxation is due to tunnel effect. In this regime *S* is **independent** of *T*.

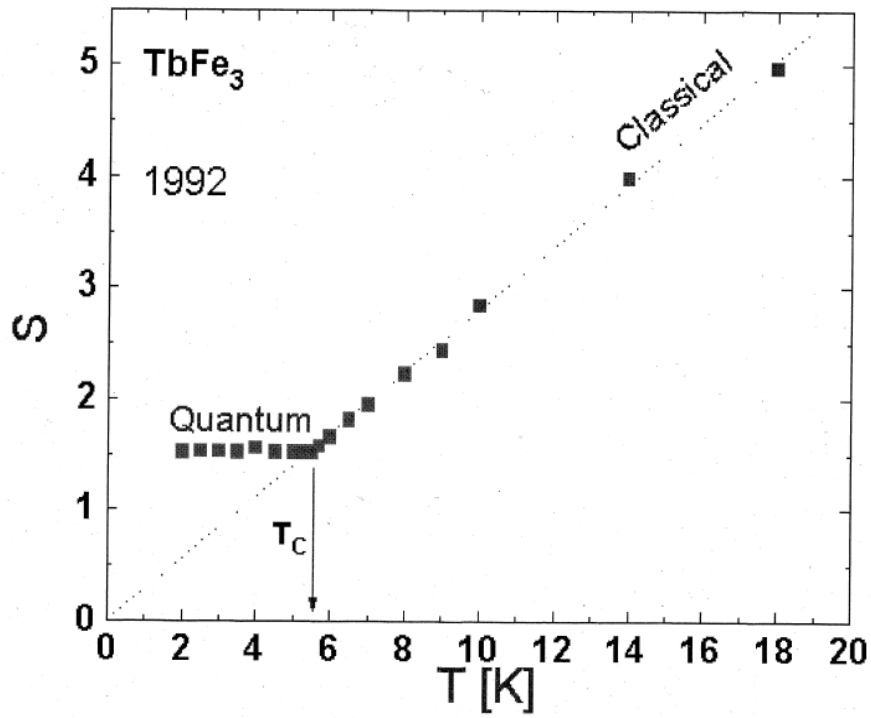

Resonant spin tunneling on molecular magnets (MM)

- Molecular magnets behave as SDP.
- Their magnetic moment ***M*** is a quantum object: it verifies the commutation relation

$$[M_l, M_j] = 2i\mu_B \epsilon_{ljk} M_k$$

which yields

$$M_l M_j - M_j M_l \sim \mu_B \epsilon_{ljk} M_k$$

$|M| \sim \mu_B$ Quantum

$|M| \gg \mu_B$ Classical

Empirically, the magnetic moment is considered to behave quantumly if $|M| \leq 1000\mu_B$ holds.

$$\mathcal{H}_A = -DS_z^2 + ES_x^2$$

M(H,T) univocally determined by D and E

UNIVERSITAT DE BARCELONA

Resonant spin tunneling on MM

- Application of an external field: adds a Zeeman term $\sim \vec{M} \cdot \vec{H}$
  Longitudinal component of the field (***H*** // easy axis) ⟹ Moves the levels.
  Transverse component of the field (***H*** ⊥ easy axis) ⟹ Allows tunnel effect.

- The tunnel effect is possible for certain values of the field: the **resonant fields.**

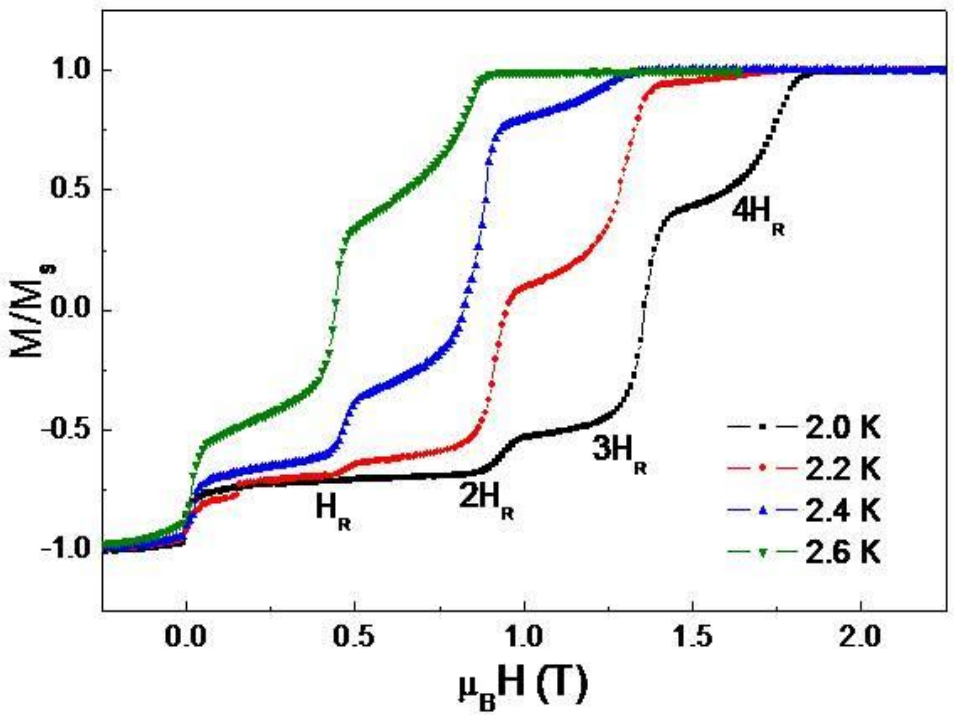

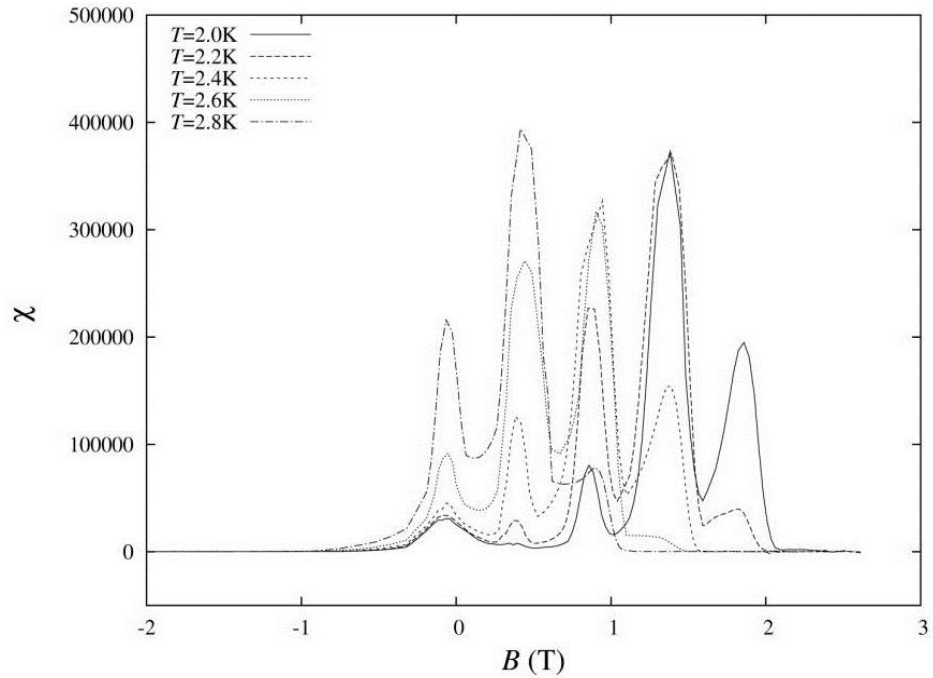

UNIVERSITAT DE BARCELONA

MILESTONES TIMELINE

1896	Zeeman effect (1)
1922	Stern–Gerlach experiment (2)
1925	The spinning electron (3)
1928	Dirac equation (4)
	Quantum magnetism (5)
1932	Isospin (6)
1940	Spin–statistics connection (7)
1946	Nuclear magnetic resonance (8)
1950s	Development of magnetic devices (9)
1950–1951	NMR for chemical analysis (10)
1951	Einstein–Podolsky–Rosen argument in spin variables (11)
1964	Kondo effect (12)
1971	Supersymmetry (13)
1972	Superfluid helium-3 (14)
1973	Magnetic resonance imaging (15)
1975–1976	NMR for protein structure determination (16)
1978	Dilute magnetic semiconductors (17)
1988	Giant magnetoresistance (18)
1990	Functional MRI (19)
	Proposal for spin field-effect transistor (20)
1991	Magnetic resonance force microscopy (21)
1996	Mesoscopic tunnelling of magnetization (22)
1997	Semiconductor spintronics (23)

Quantum magnetic deflagration

Avalanche ignition produced by SAW:

Surface Acoustic Waves (SAW) are low frequency acoustic phonons (below 1 GHz)

Coaxial cable connected to an Agilent microwave signal generator

Change in magnetic moment registered in a rf-SQUID magnetometer

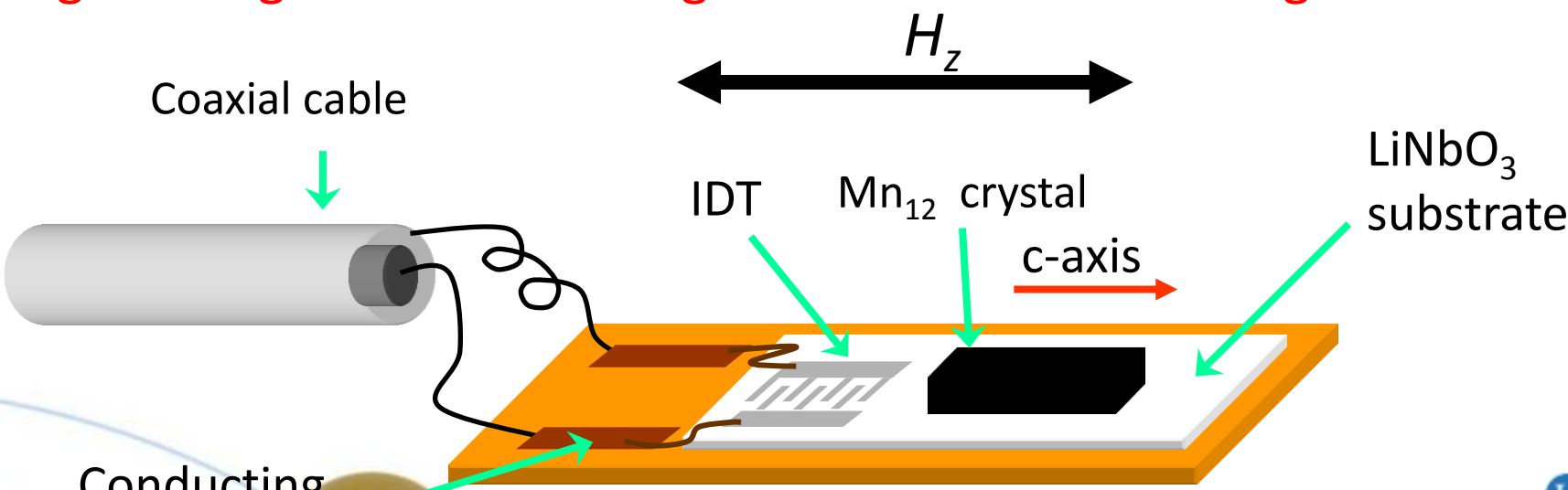

Quantum magnetic deflagration

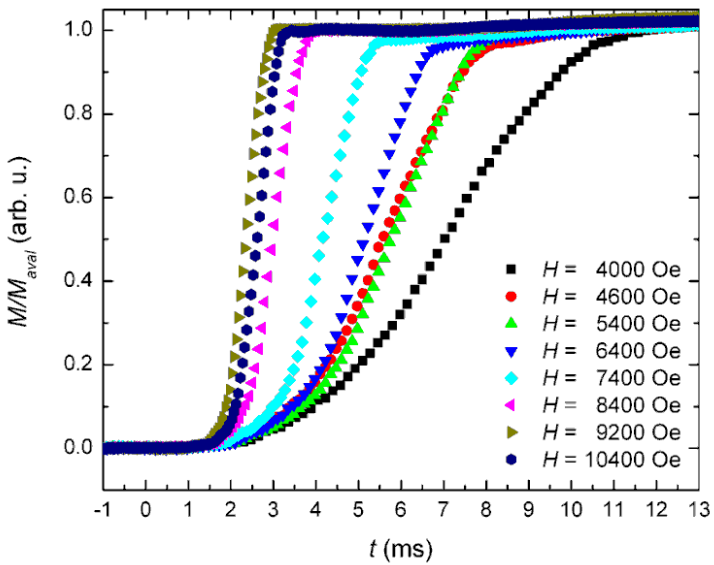

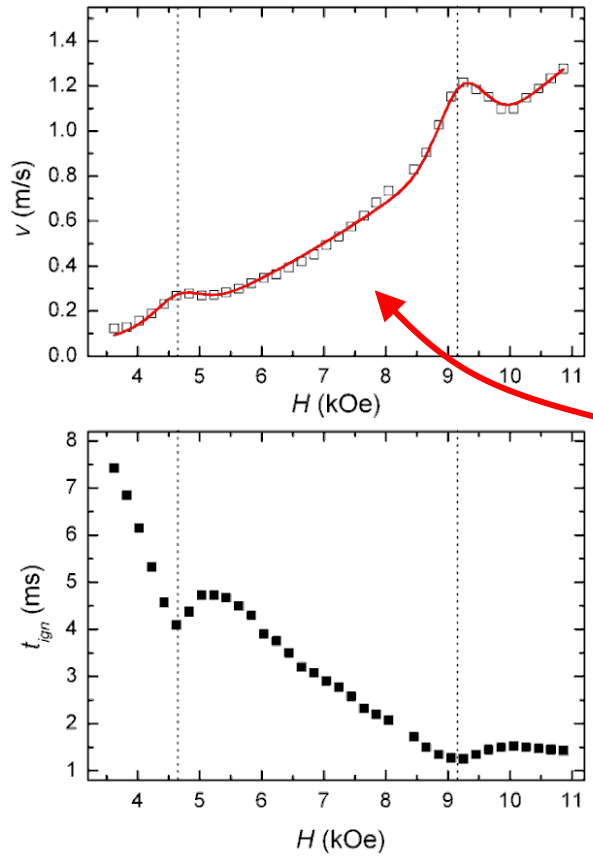

$$v = \sqrt{\frac{\kappa}{\tau_0}} \exp\left(-\frac{U(H)}{2k_B T_f}\right)$$

This velocity is well fitted:

$\kappa = 0.8 \cdot 10^{-5}$ m^2/s

T_f (H = 4600 Oe) = 6.8 K

T_f (H = 9200 Oe) = 10.9 K

- The speed of the avalanche increases with the applied magnetic field
- At resonant fields the velocity of the flame front presents peaks.
- The ignition time shows peaks at the magnetic fields at which spin levels become resonant.

UNIVERSITAT DE BARCELONA

Quantum Magnetic Deflagration

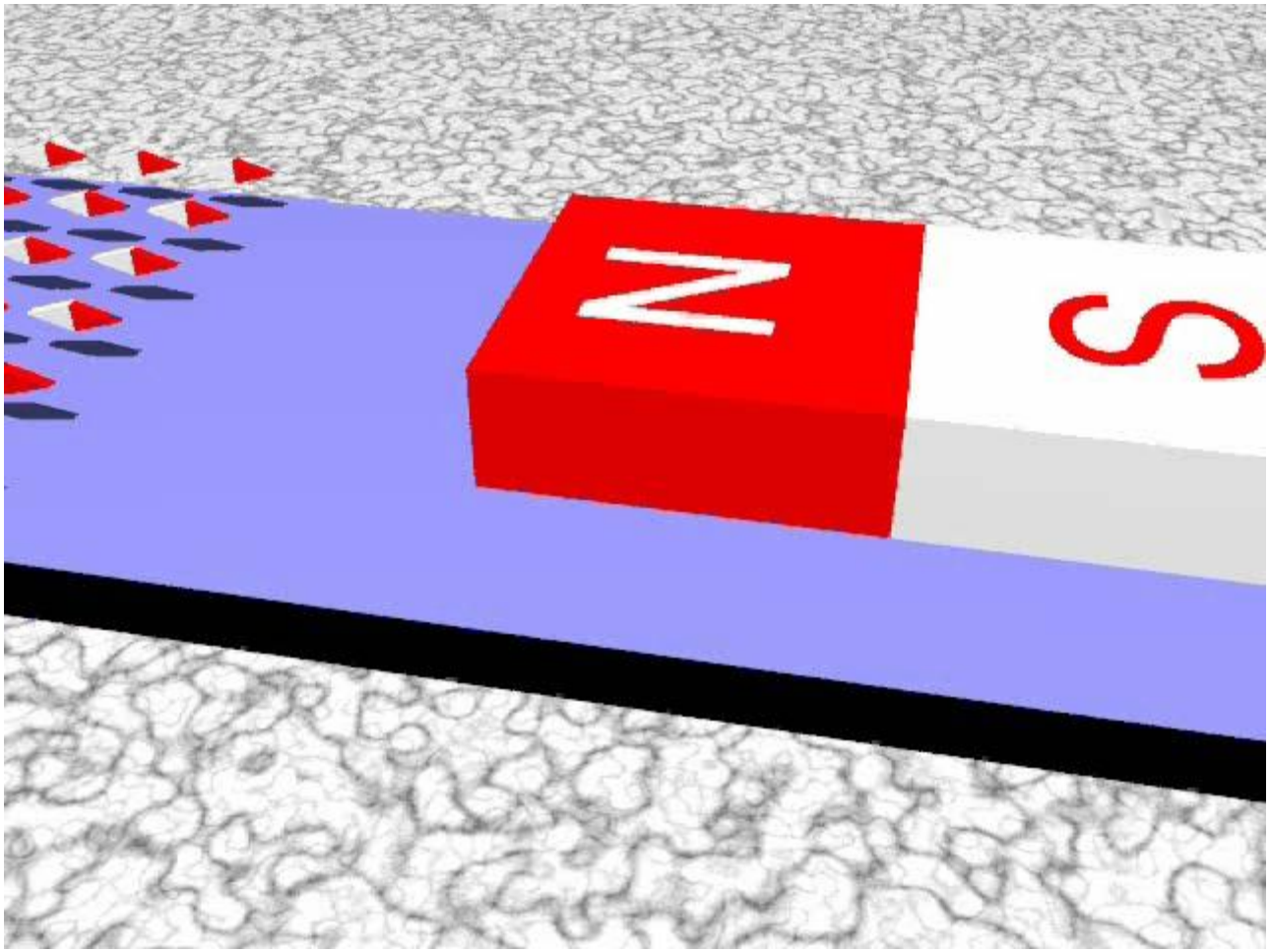

Quantum Magnetic Deflagration

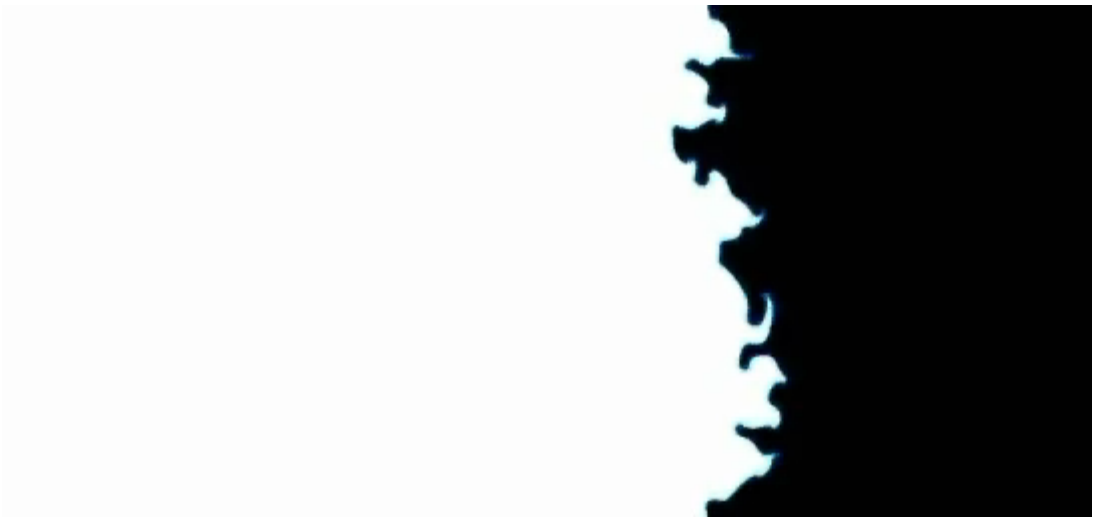

Quantum Magnetic Deflagration

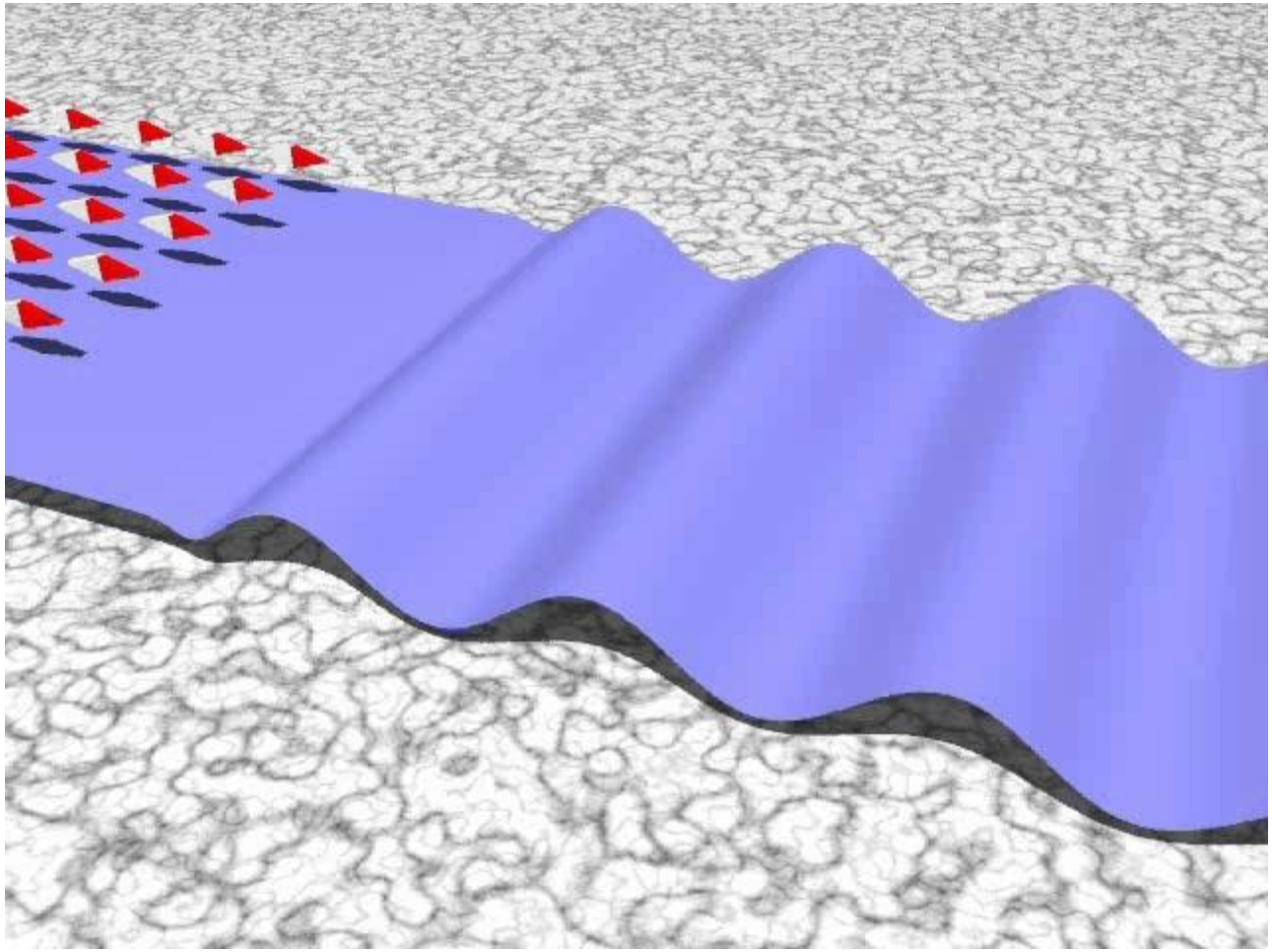

Superradiance

This kind of emission (SR) has characteristic properties that make it different from other more common phenomena like luminescence

Luminescence

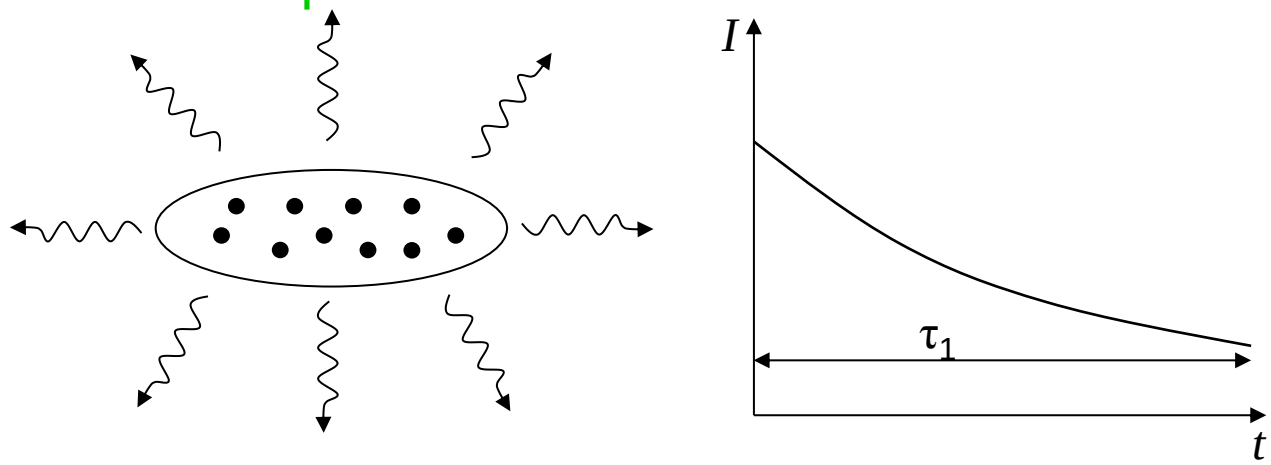

Superradiance

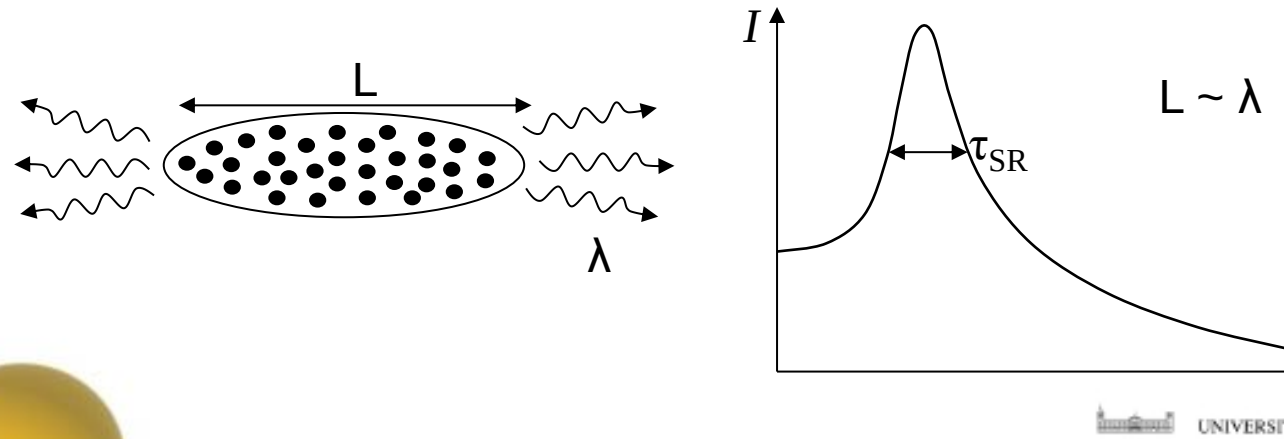

Superradiance

All spins decay to the fundamental level coherently, with the emission of photons.

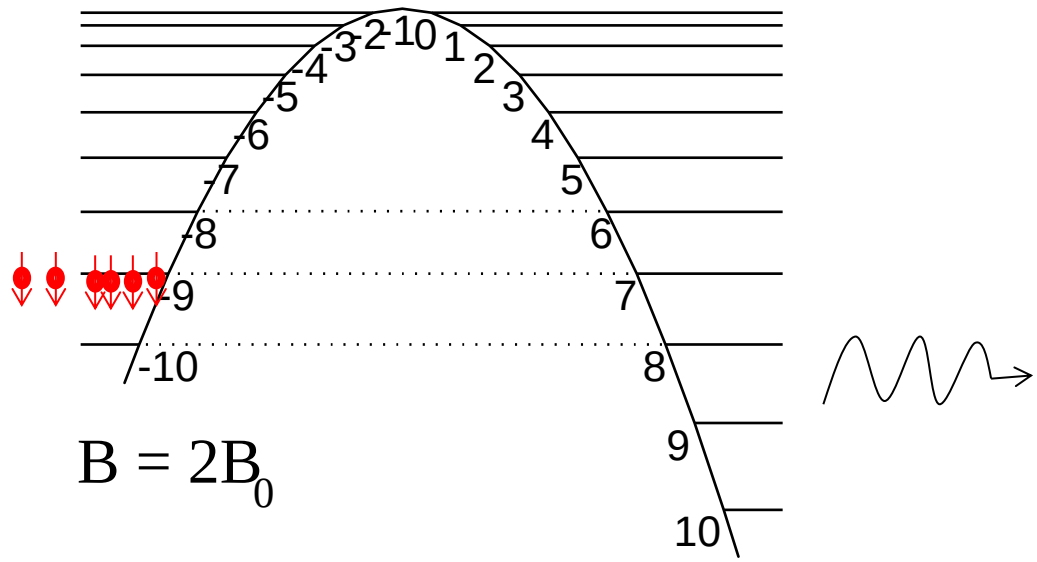

Superradiance

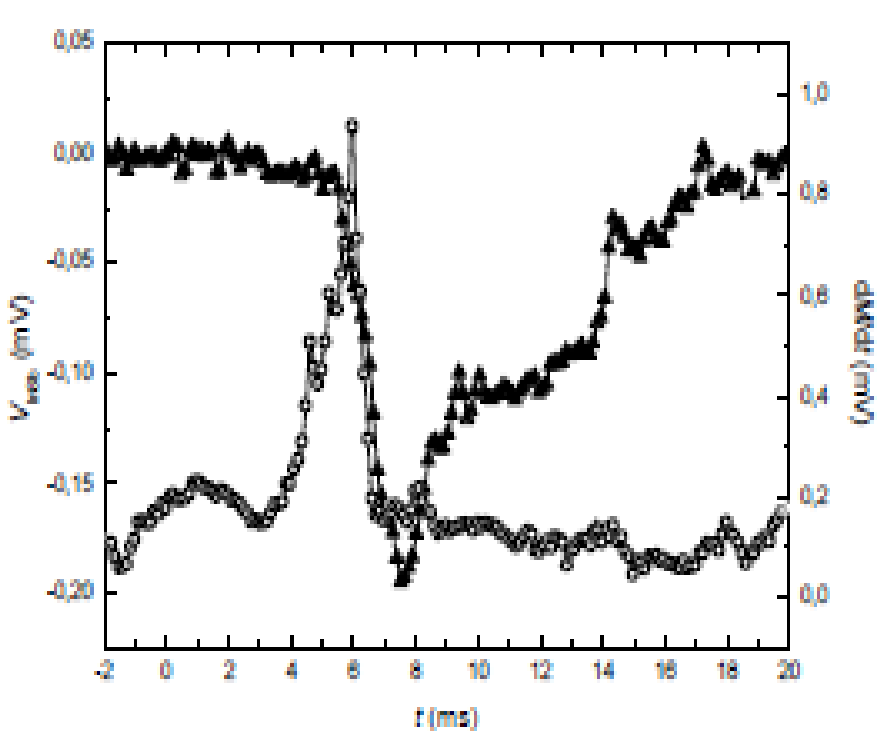

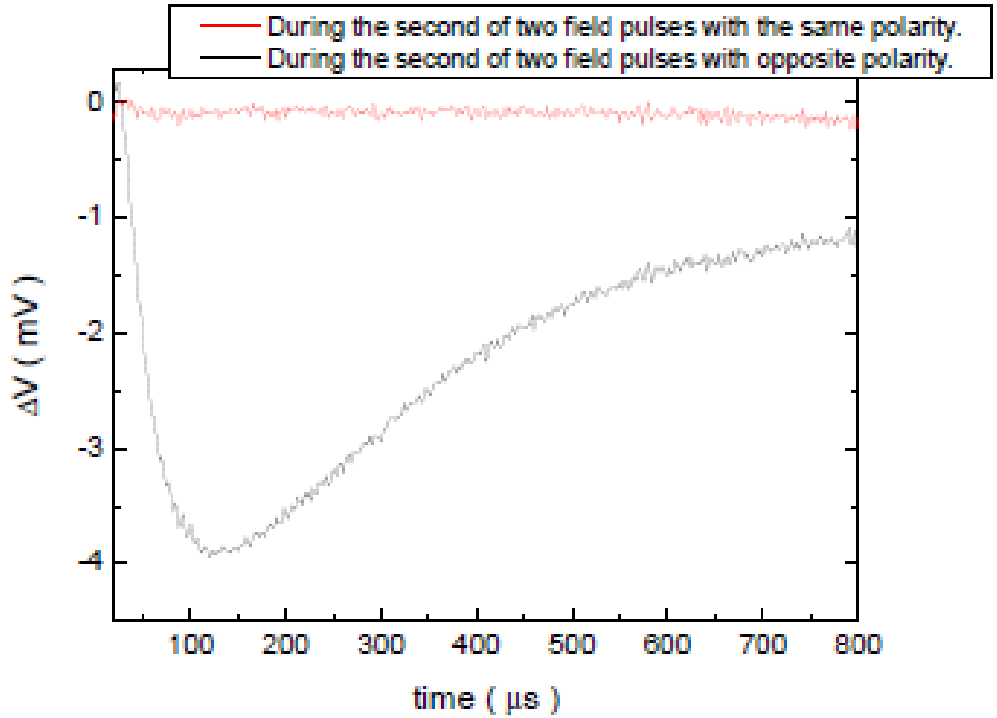

A. Hernández-Mínguez *et al*. Europhys. Lett. **69**, 270 (2005).

Rotational Doppler Effect

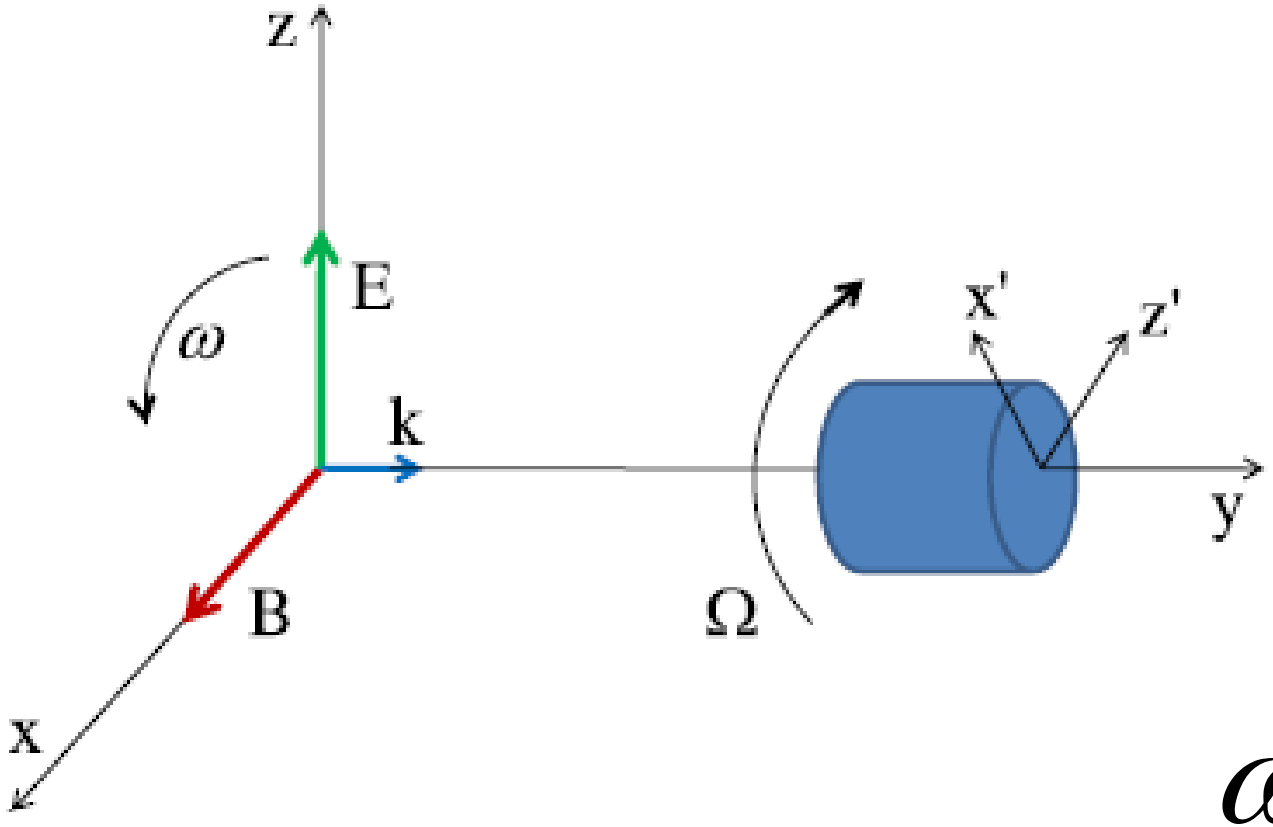

$$\omega' = \omega \pm \Omega$$

EPR Results

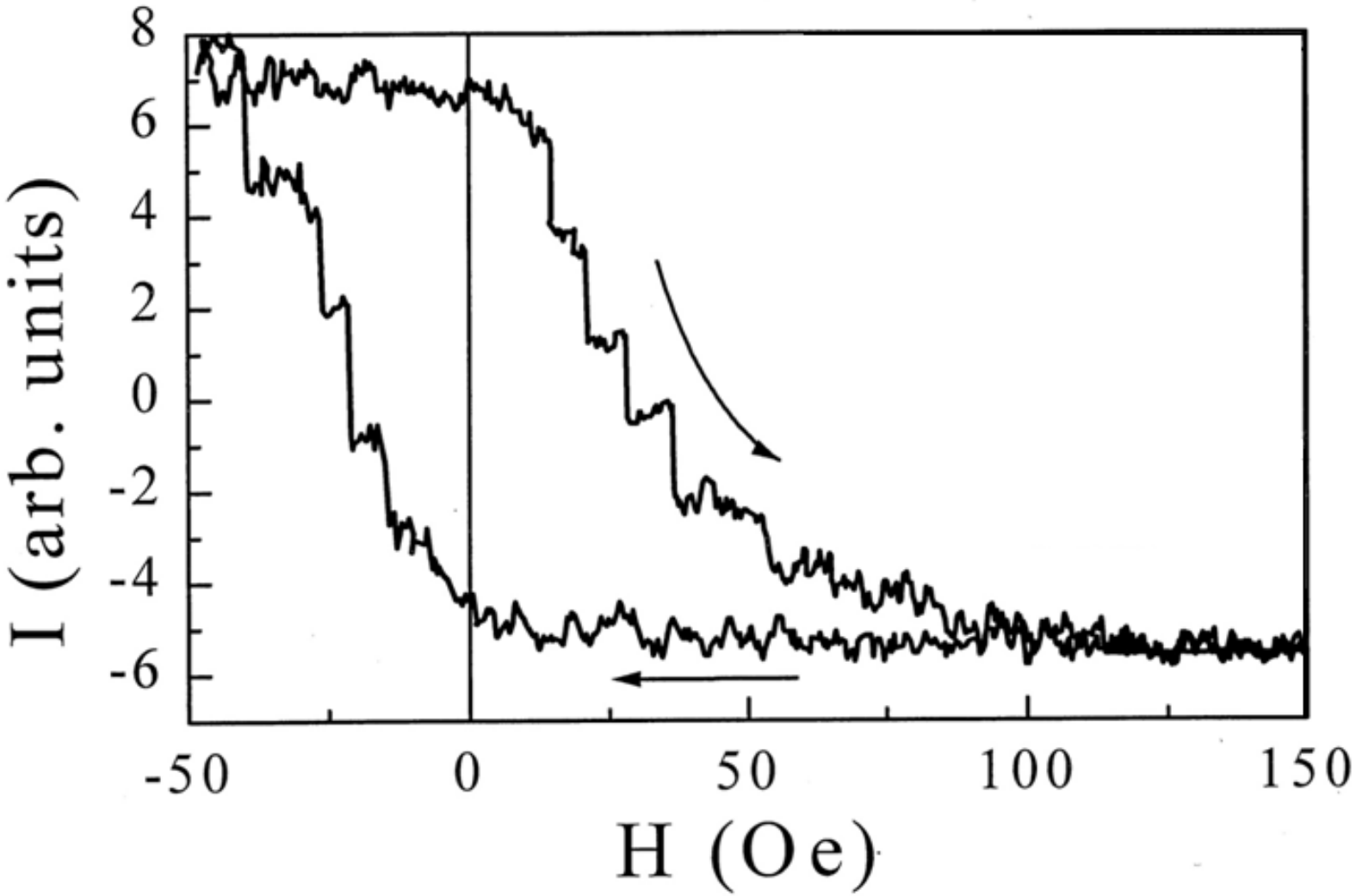

Rotational Doppler Effect

$$\omega_{FMR} = \omega_0 + \gamma H \qquad \gamma = \frac{2\mu_B}{\hbar}$$

$$\omega' = \omega \pm \Omega \qquad \Omega = \frac{n\hbar}{I}$$

$$\gamma H_n = \omega - \omega_0 \pm \frac{n\hbar}{I}$$

$$\Delta H = H_{n+1} - H_n = \cdots = \frac{\hbar}{\gamma I} = \frac{\hbar^2}{2\mu_B I}$$

measured $\Delta H \sim 2.5 Oe$

produced by $r \sim 1\ nm$ particles

Magnetic Vortices (MV): Introduction

Vortex State

- The spin field splits into two well-differentiated structures: 1) the vortex core consisting of a uniform out-of-plane spin component (spatial extension about the exchange length) and 2) the curling magnetization field (in-plane spin component), characterized by a non-zero vorticity value.
- The application of an in-plane magnetic field yields the displacement of the vortex core perpendicularly to the field direction.
- The vortex shows a special vibrational mode (called gyrotropic mode) consisting of the displacement of the vortex core as a whole, following a precessional movement around the vortex centre. Its characteristic frequency belongs to the subGHz range.

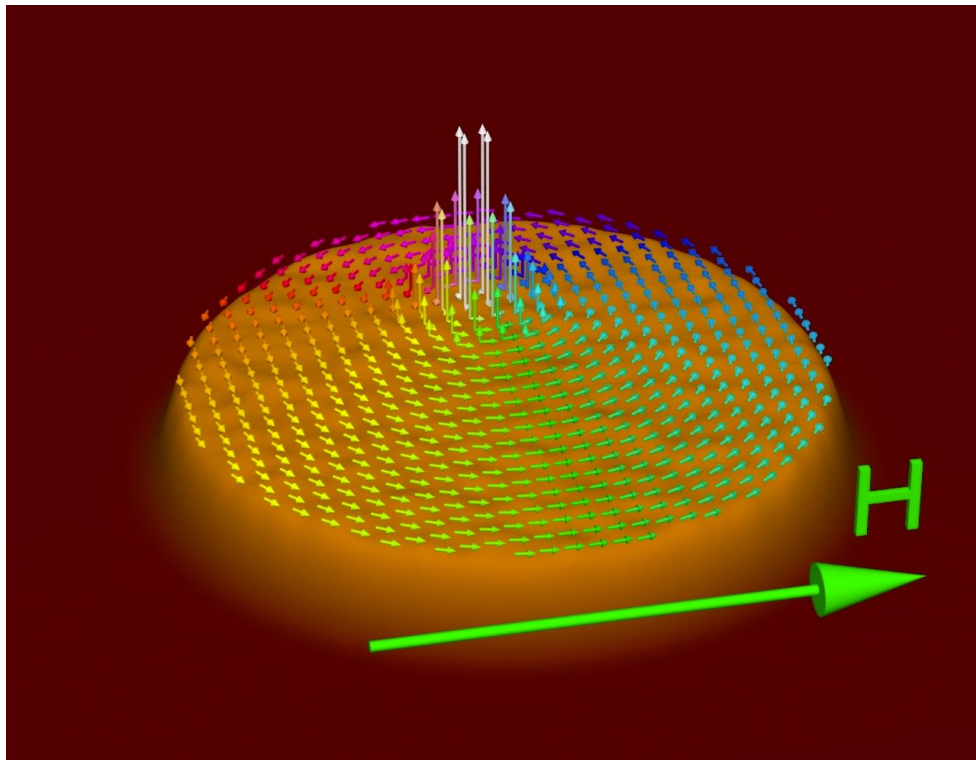

Experimental set-up

We have studied several arrays of permalloy ($Fe_{19}Ni_{81}$) disks with diameter $2R$ = 1.5 μm and different thickness (L = 60, 95 nm) under the application of an in-plane magnetic field up to 0.1 T in the range of temperatures 2-300 K. Samples were prepared stacking four 5x5 mm^2 arrays with parallel sides.

UNIVERSITAT DE BARCELONA

MV: Magnetic Characterization

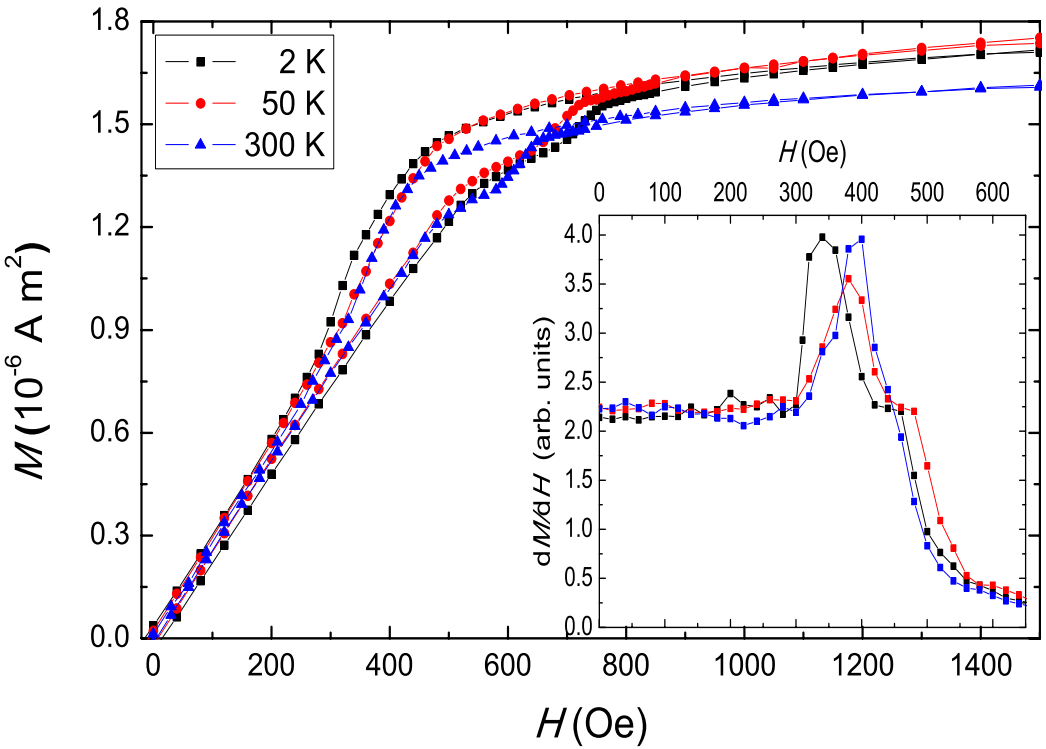

Hysteresis loop of a sample with thickness L = 95 nm.

The vortex linear regime in the ascending branch should extend from H=-300 Oe to 500 Oe (at least) in the L = 95 nm sample. Analogous behaviour has been observed in the other sample.

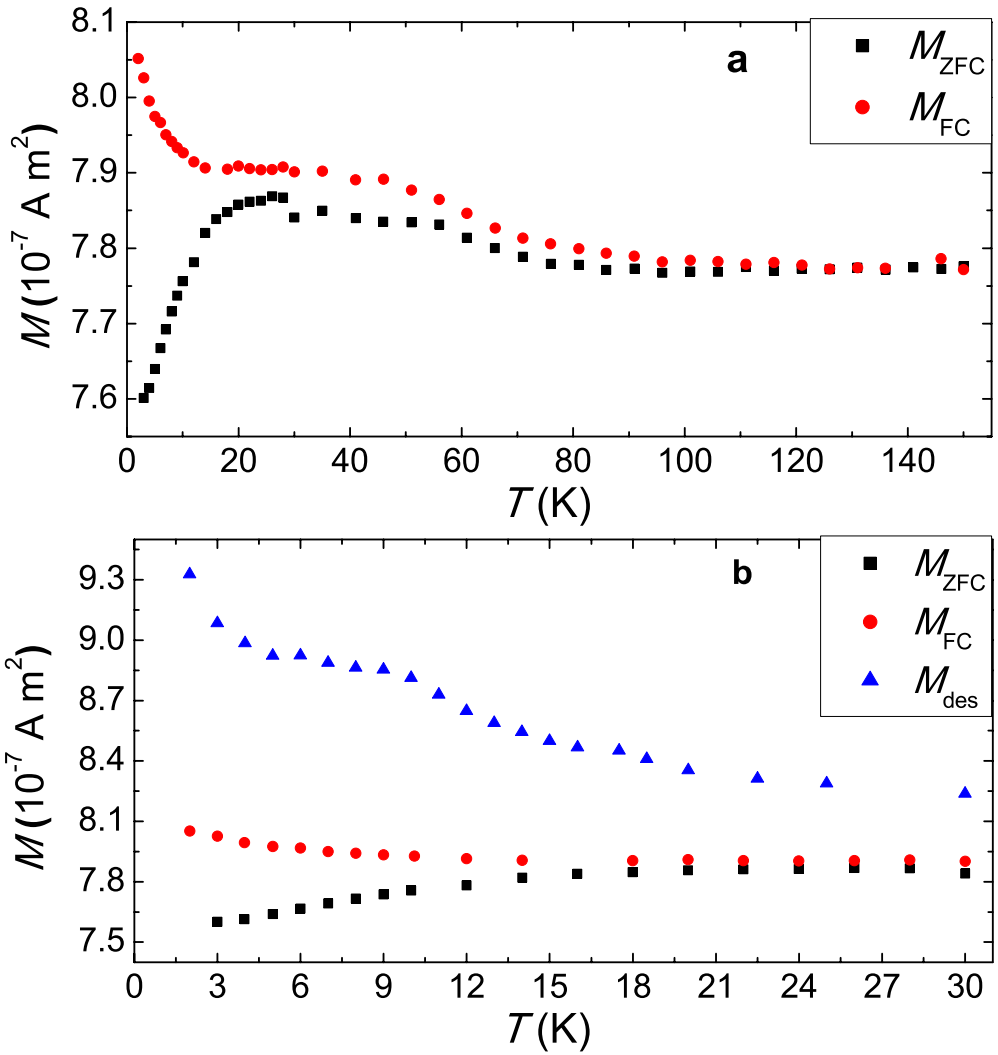

a) ZFC-FC curves for an applied magnetic field H = 300 Oe (L = 95 nm). b) Isothermal magnetic measurements along the descending branch, $M_{des}(H)$, from the SD state (H = 0.1 T) to H = 300 Oe (L = 95 nm).

MV: Relaxation Experiments

Relaxation mesurements of magnetic vortices from the metastable states of the descending branch at H = 0 to the equilibrium state (which corresponds to M=0) for both samples.

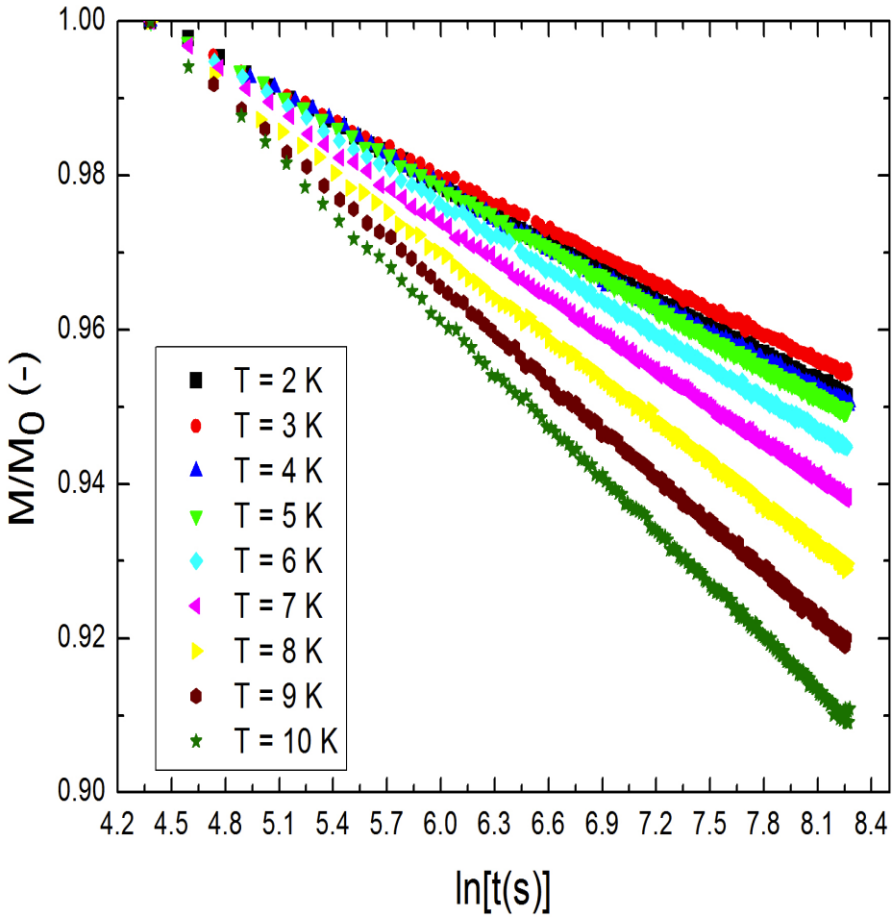

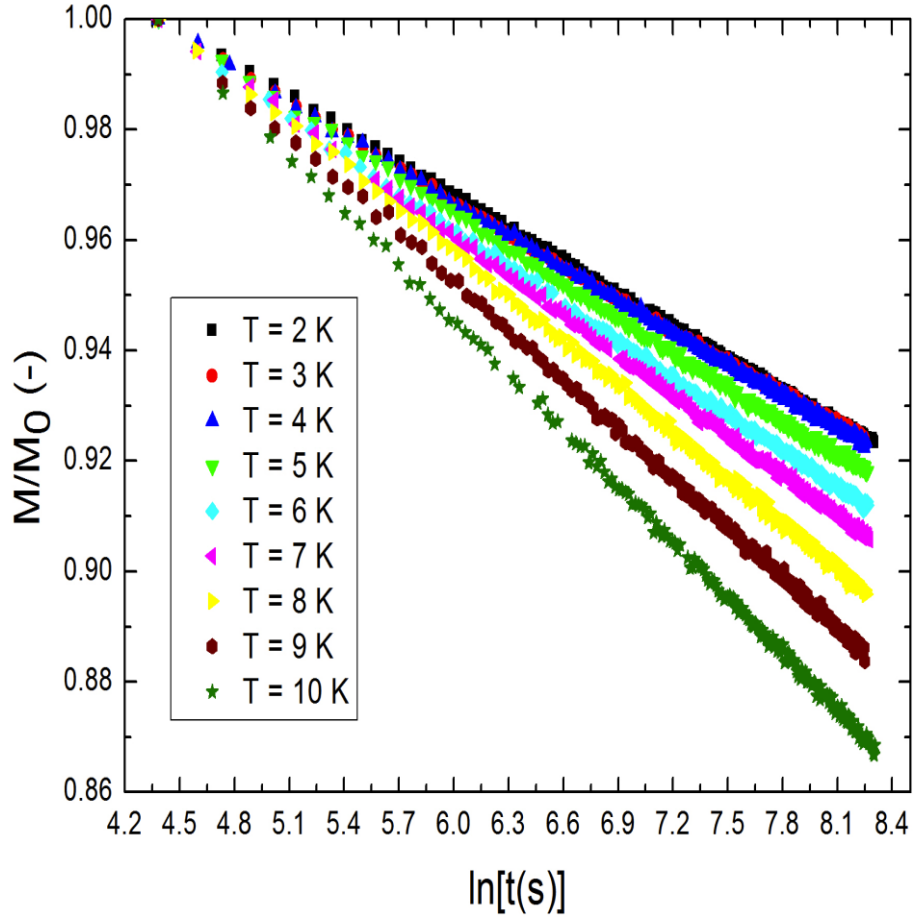

Normalized relaxation measurements for samples L = 60 nm (left) and L = 95 nm (right). M_0 corresponds to the initial point of the relaxation.

UNIVERSITAT DE BARCELONA

MV: Viscosity and conclusions (pt 1)

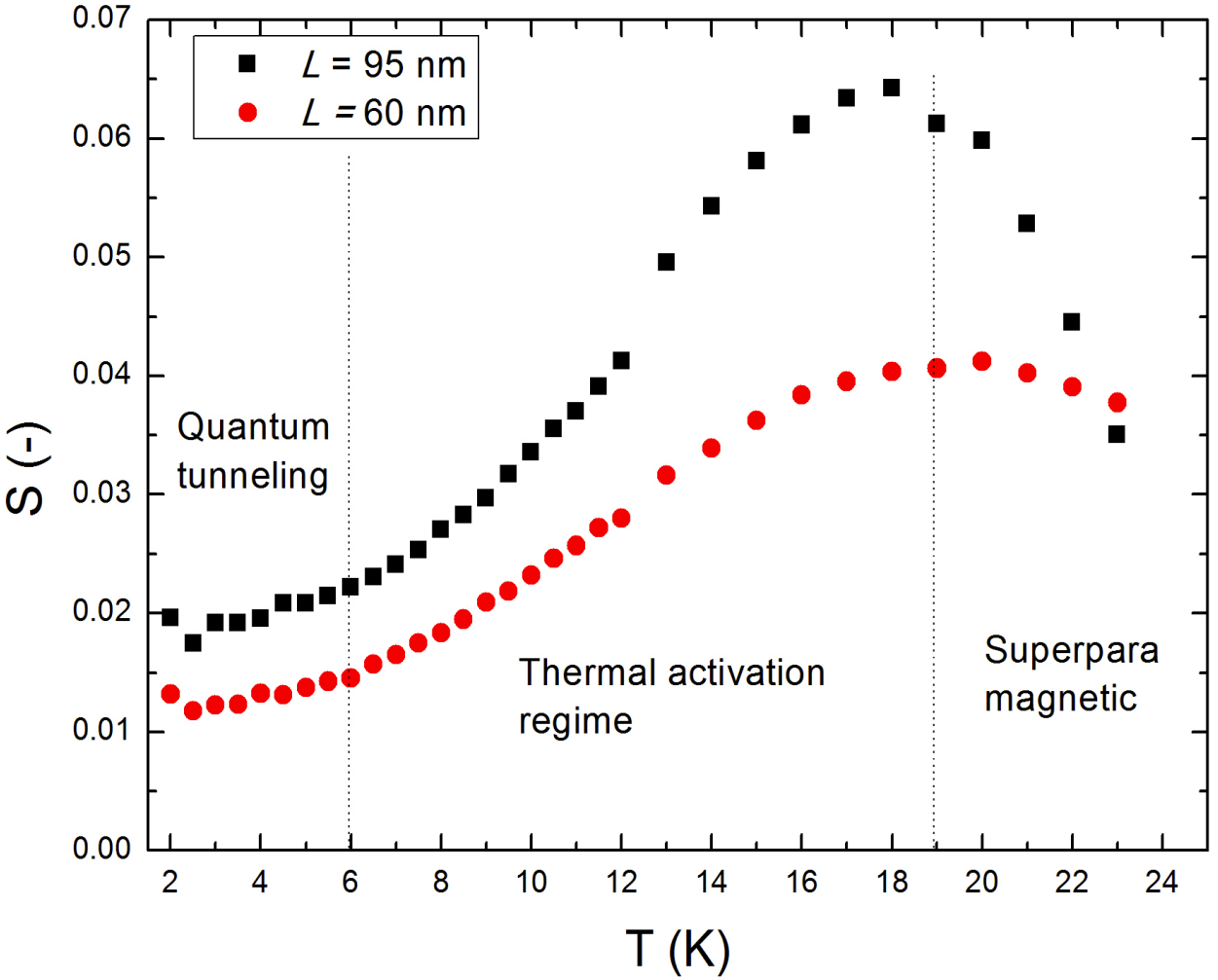

Magnetic viscosity *S* versus temperature *T* for both samples.

Below *T* = 6 K, magnetic viscosity reaches a plateau with non-zero value.

Conclusions:

- Logarithmic time dependence of the magnetization implies a broad distribution of energy barriers in our system.

- Thermal activation of energy barriers dies out in the limit T → 0. Observation that magnetic viscosity *S*(*T*) tends to a finite value different from zero as *T* → 0 indicates that relaxations are non-thermal in this regime.

UNIVERSITAT DE BARCELONA

MV: Conclusions (pt 2)

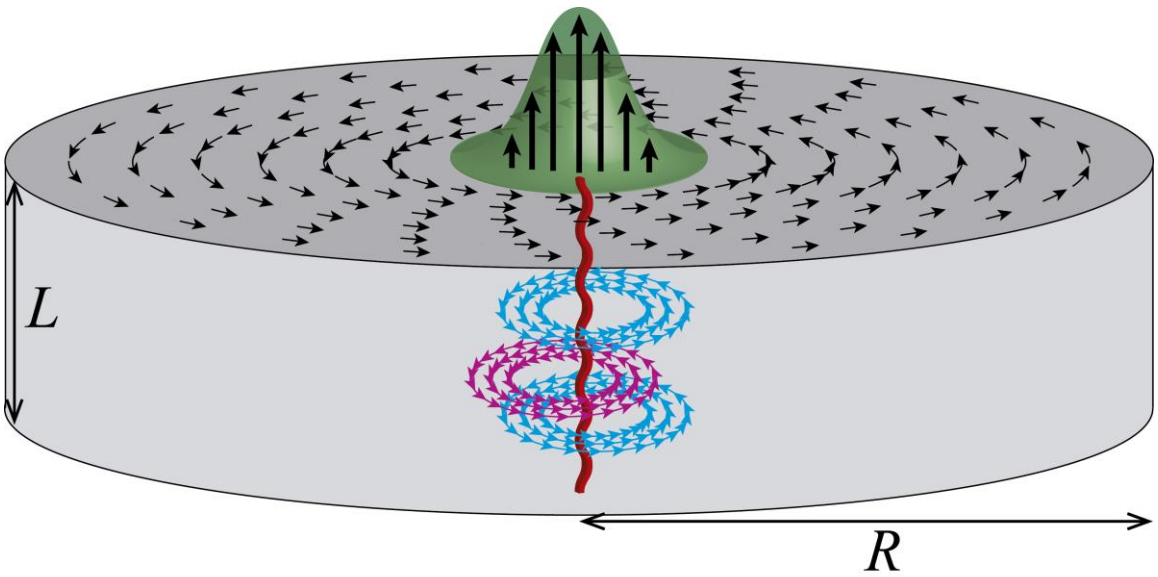

Conclusions:

•The presence of structural defects in the disks could be a feasible origin of the energy barriers. We consider them to be capable of pinning the vortex core, when the applied magnetic is swept, in a non-equilibrium position.

•The elastic nature of the VC line allows an spatial deformation of this structure along the cylindrical axis. The observed quantum depinning appears to be due to underbarrier QT transitions of small segments of the VC line.

UNIVERSITAT DE BARCELONA

Type I SC: Topological hysteresis

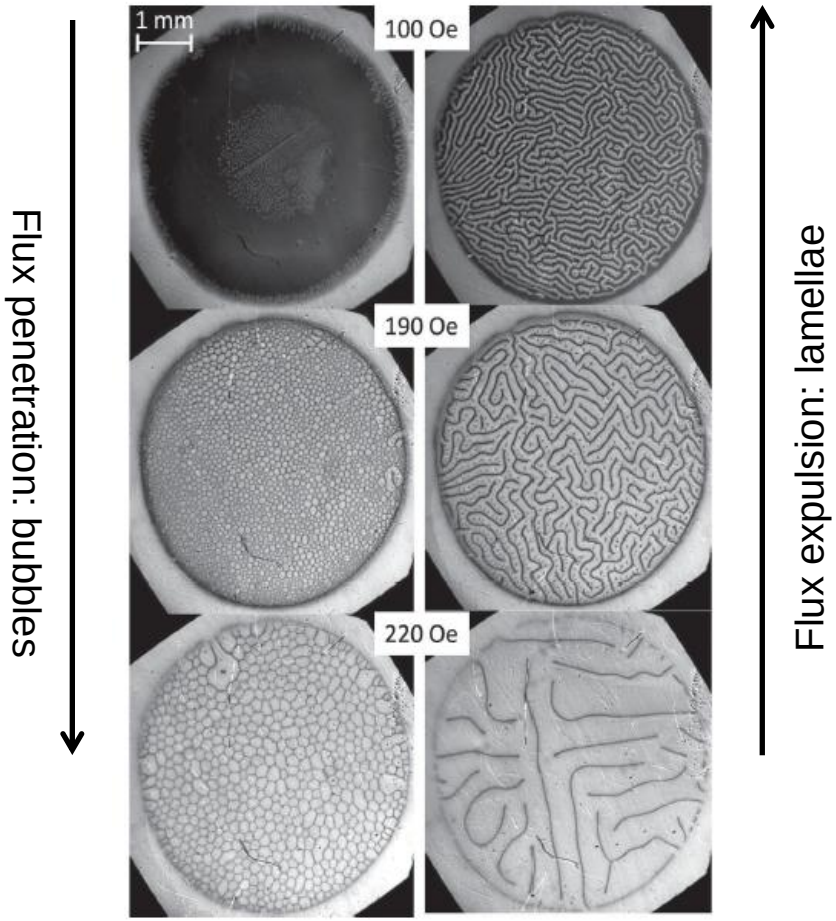

There is a **GEOMETRICAL BARRIER** controlling both the **penetration** and the **expulsion** of **magnetic flux** in the **intermediate state.** It is the responsible for both the **intrinsic irreversibility** of a **pure defect-free samples** and the formation of **different flux patterns.**

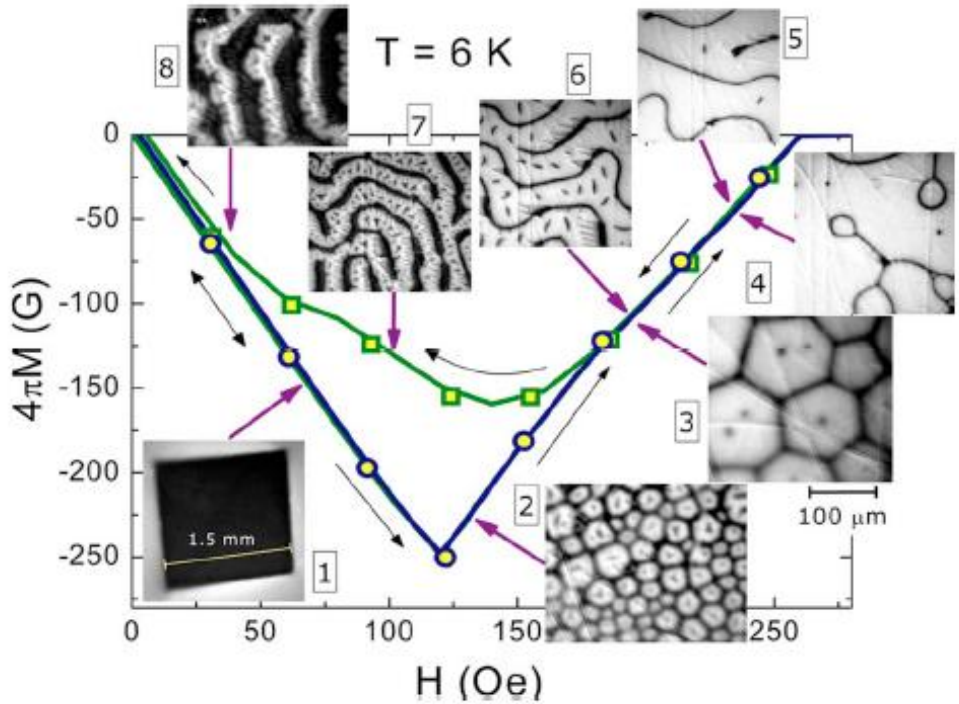

Different flux structures appear in the Intermediate state depending on the magnetic history: **Tubes/bubbles** are formed during magnetic field **penetration** and **labyrinthic patterns** appear upon **expulsion**

UNIVERSITAT DE BARCELONA

Type I SC: Magnetic relaxation

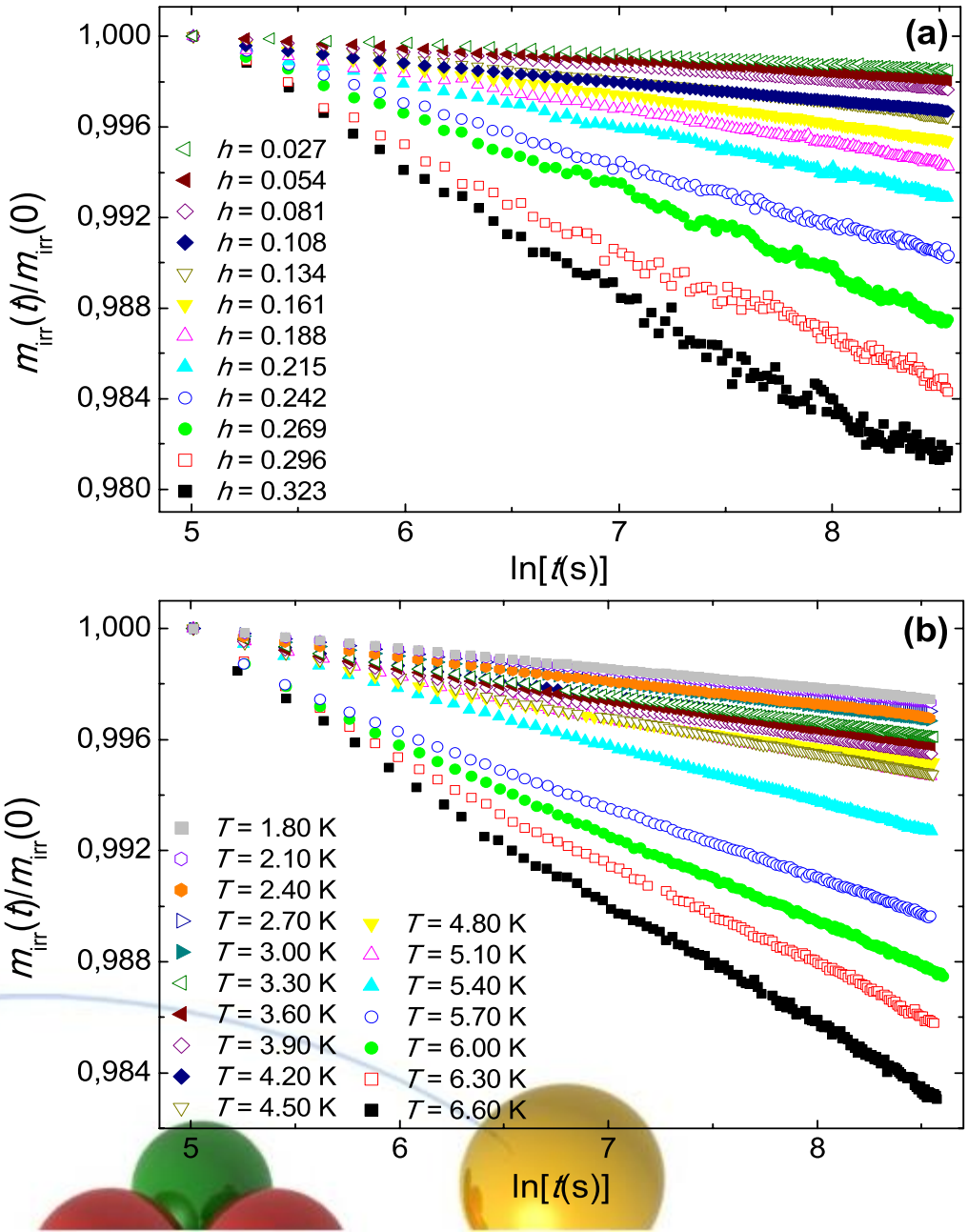

Relaxation mesurements of a Pb sample from the metastable states of the descending branch for different reduced fields *h* in steps of 0.027 at *T*=2 K (a) and at different *T* for the fixed reduced field *h*=0.10 (b).

We observe a perfect logarithmic time dependence of m(t) for several T and h:

$$m_{irr}(t) = m(t) - m_{eq},$$

$$m_{irr}(t) = m_{irr}(0)[1 - S\ln(t)]$$

This law holds for any system having a **broad distribution of energy barriers** as the source of its metastability

UNIVERSITAT DE BARCELONA

Type I SC: N-SC Interfaces

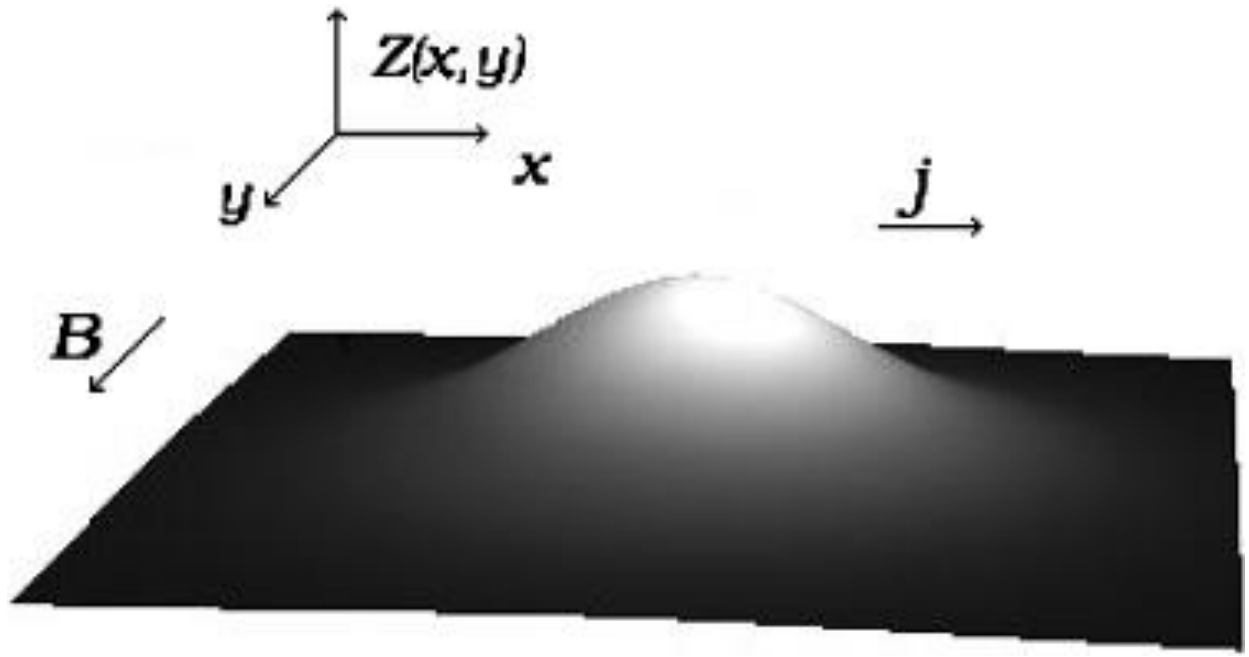

Interface between normal and superconducting regions in a type-I superconductor, pinned by a planar defect in the *XY* plane. Transport current parallel to the interface controls the energy barrier. Depinning of the interface occurs through quantum nucleation of a critical bump.

Quantum tunneling of N-SC interfaces

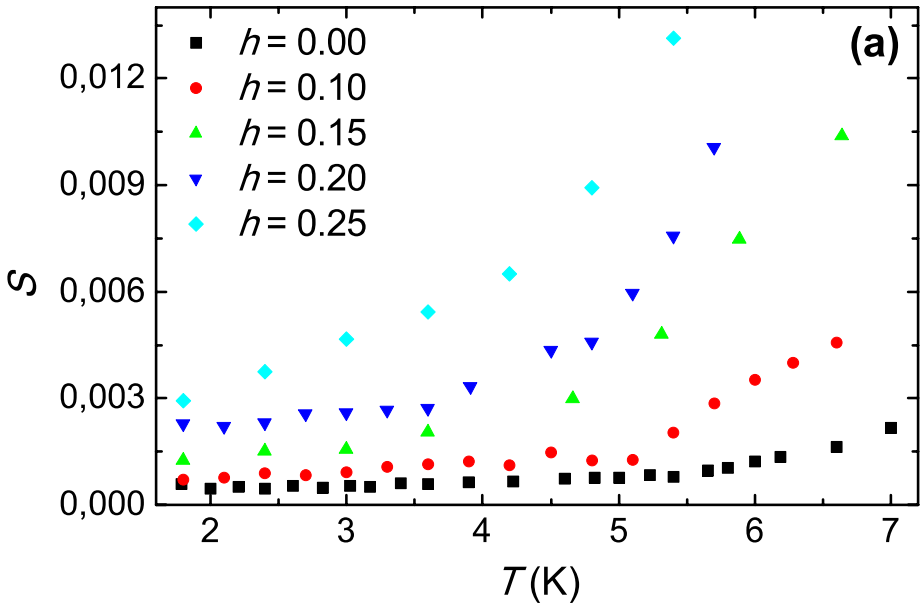

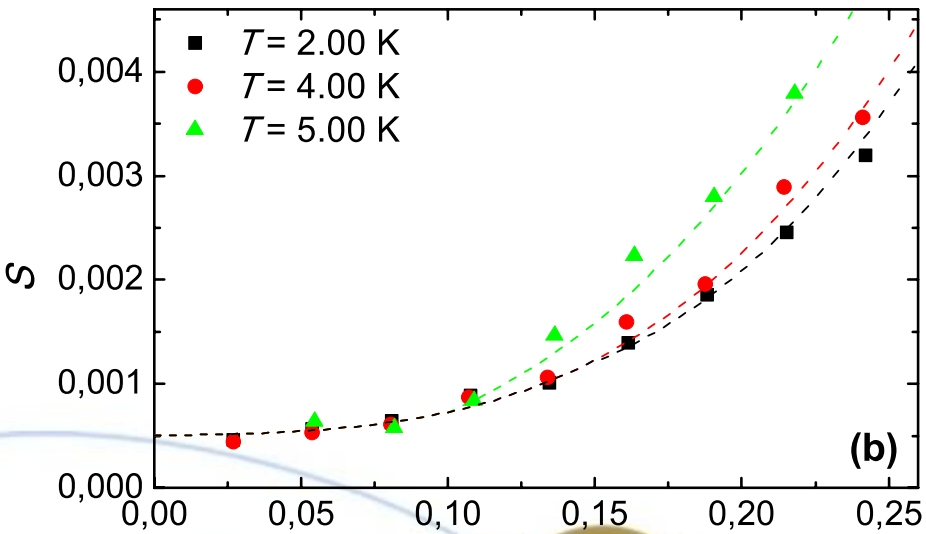

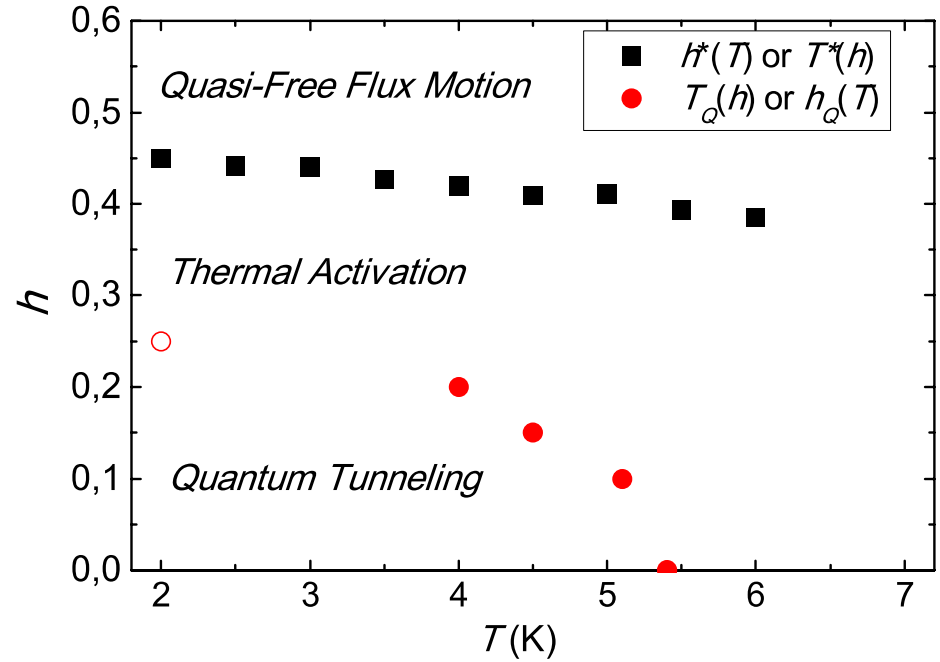

Left figure: Temperature dependence of the magnetic viscosity for different reduced fields (a) and reduced magnetic field dependence of *S* at different *T* (b). **Right figure:** Reduced magnetic field vs. *T* phase diagram showing the different dynamical regimes.

UNIVERSITAT DE BARCELONA

References

[1] E. M. Chudnovsky, J. Tejada, *Macroscopic Quantum Tunneling of the Magnetic Moment* (Cambridge Univ. Press, 1998).
[2] J.R. Friedman, M.P. Sarachik, J. Tejada and R. Ziolo. Phys. Rev. Lett. 76, 3830–3833 (1996).
[3] A. Hernández-Mínguez et al. Phys. Rev. Lett. 95, 217205 (2005).
[4] F. Macià et al. Phys. Rev. B 79, 092403 (2009).
[5] S. Vélez et al. Phys. Rev. B 81, 064437 (2010).
[6] W. Decelle et al. Phys. Rev. Lett. 102, 027203 (2009).
[7] J. Tejada, R. D. Zysler, E. Molins and E. M. Chudnovsky. Phys. Rev. Lett. 104, 027202 (2010).
[8] R. Zarzuela, S. Vélez, J.M. Hernandez, J. Tejada and V. Novosad. Phys. Rev. B 85, 180401(R) (2012).
[9] E.M. Chudnovsky, S. Vélez, A. García-Santiago, J.M. Hernandez and J. Tejada. Phys. Rev. B 83, 064507 (2011).

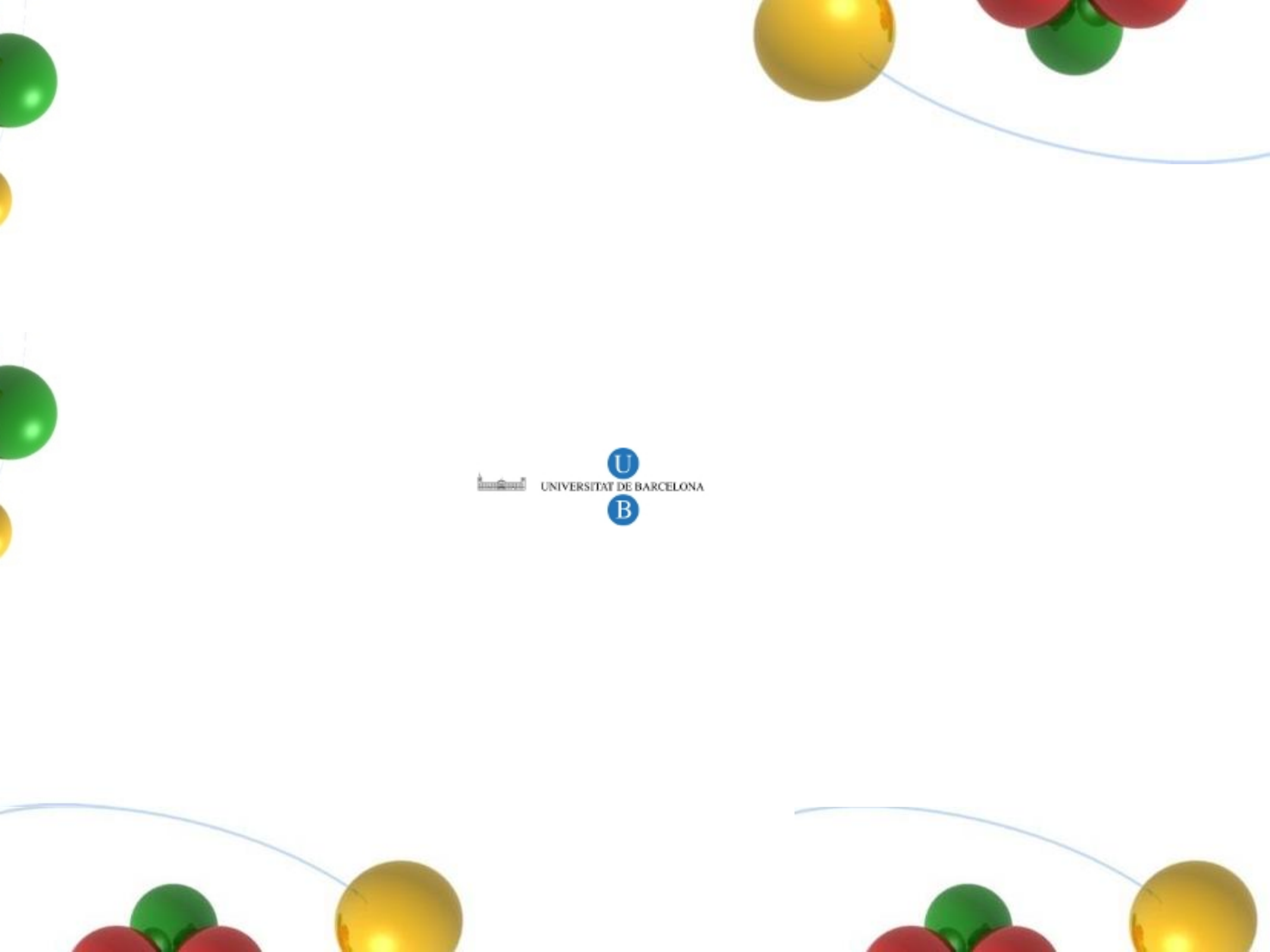
UNIVERSITAT DE BARCELONA